IFT/01-06
SINP/TH/00-33
TIFR/TH/01-06
hep-ph/0103161

Supersymmetric lepton flavour violation in a linear collider: the role of charginos

M. Guchait*

Saha Institute of Nuclear Physics
Bidhan Nagar, Calcutta - 700064, India.

J. Kalinowski†

Instytut Fizyki Teoretycznej, Uniwersytet Warszawski
Hoża 69, 00681 Warszawa, Poland.

Probir Roy‡

Tata Institute of Fundamental Research
Homi Bhabha Road, Mumbai-40005, India.

Abstract

The occurrence of a significant amount of supersymmetric lepton flavour violation at laboratory energies, through $\tilde{\nu}_\mu - \tilde{\nu}_\tau$ mixing, has become a realistic possibility in the wake of the super-Kamiokande atmospheric neutrino result. This effect can be observed in an e^+e^- linear collider with the distinct final state $\tau\mu + jets + \not{E}_T$. We show that the pair production of charginos can make an important contribution to this process and has to be taken into account in addition to that of sneutrinos or charged sleptons. Some case studies are presented with CM energies of 500 and 800 GeV and integrated luminosities of 50, 500 and 1000 fb^{-1}.

*guchait@tnp.saha.ernet.in
†Jan.Kalinowski@fuw.edu.pl
‡probir@tifr.res.in

1 Introduction.

The results of the super-Kamiokande atmospheric neutrino experiment [1] provide compelling evidence of lepton flavour violation. Combined with recent data from reactor antineutrino studies [2], these strongly suggest a large near-maximal mixing ($\theta_{\nu_\mu\nu_\tau} \sim \pi/4$) and consequent oscillations between very lightly massive mu and tau neutrinos. The latest analysis implies $\Delta m^2 \equiv |m^2_{\nu_\mu} - m^2_{\nu_\tau}| \sim 3 \times 10^{-3}$ eV^2 and $\sin^2 2\theta_{\nu_\mu\nu_\tau} > 0.88$. Unless the two neutrinos are closely degenerate, their masses may be expected to have the same order of magnitude as their mass difference. The long-standing deficit of solar neutrinos [3] may also be explained by neutrino oscillations, though the presence of $\nu_e \to \nu_\mu$ or $\nu_e \to \nu_\tau$ oscillations at a high level is still an open question.

Neutrino oscillations imply the violation of individual lepton flavour numbers and raise an interesting possibility of observing processes with a violation of lepton flavour between two charged leptons, such as $\mu \to e\gamma$, or $\tau \to \mu\gamma$ [4, 5]. In the Standard Model these processes are strongly suppressed due to the GIM mechanism. However, in the supersymmetric extension of the Standard Model, new mechanisms with virtual superpartner loops may enhance [5] these rare decay processes. Of course, once superpartners are discovered, it will be possible to probe lepton flavour violation directly in their production and decay processes [6]. For example, it has been demonstrated that sneutrino or charged slepton pair production at future e^+e^- (and/or $\mu^+\mu^-$) colliders may provide a more powerful tool to search for supersymmetric lepton flavour violation (SLFV) than the said rare decay processes [7, 8].

In this note we point out that sneutrinos and charged sleptons may not only be directly pair-produced in e^+e^- collisions, but can also be decay products of other supersymmetric particles, like charginos and neutralinos, decaying via cascades. The latter may contribute to the signal as well as background for SLFV processes. Therefore, a detailed account of these is needed in assessing the sensitivity of future colliders to SLFV. We find that off-diagonal chargino pair-production, overlooked earlier, can make a significant contribution to the SLFV signal already at $\sqrt{s} = 500$ GeV, and further that the role of neutralinos in decay chains is quite important and needs to be taken into account. At a CM energy of 800 GeV the diagonal pair production of the heavier chargino may also need to be included. We provide detailed studies of the SLFV signal at these two energies for two representative points of the parameter space of the MSSM. Significance contours are drawn in the parameter plane with the sneutrino mass difference as one axis and the sine of twice the sneutrino mixing angle as the other.

2 Signatures of slepton mixing

Within the framework of a seesaw mechanism [9], it is reasonable to suppose that masses and mixings in the $\nu_\mu - \nu_\tau$ system are caused by very heavy right-handed Majorana neutrinos with masses that are upwards of 10^{10} GeV. Then flavour violating mixings get radiatively induced [10] in the charged slepton and sneutrino sectors via renormalization group equations. In such a scheme a substantial $\nu_\mu - \nu_\tau$ mixing leads to [7, 11] large $\tilde{\mu}_L - \tilde{\tau}_L$ and $\tilde{\nu}_\mu - \tilde{\nu}_\tau$ mixings. In this paper we do not discuss these theories; we concentrate on the

question how well SLFV can be probed at future e^+e^- colliders in a model independent way.

For nearly degenerate sleptons, additional SLFV contributions to rare decay processes are suppressed as $\Delta m_{\tilde{l}}/m_{\tilde{l}}$ through the superGIM mechanism. As a result, constraints from the yet unobserved radiative decays $\mu \to e\gamma$, $\tau \to \mu\gamma$, $\tau \to e\gamma$ are not very stringent [4]. On the other hand, in decays of sleptons, this kind of supersymmetric lepton flavour violation is suppressed only as $\Delta m_{\tilde{l}}/\Gamma_{\tilde{l}}$ [7]. Since $m_{\tilde{l}}/\Gamma_{\tilde{l}}$ is typically of the order 10^2–10^3, one may expect spectacular signals [7, 8] for possible discovery in future e^+e^- or $\mu^+\mu^-$ collider experiments.

To be more specific, let us take a pure 2-3 intergeneration mixing between $\tilde{\nu}_\mu$ and $\tilde{\nu}_\tau$, generated by a near-maximal mixing angle θ_{23}, and let us ignore any mixings with $\tilde{\nu}_e$. This means that scalar mass matrices are not diagonal in the same basis as fermion mass matrices. For example, the scalar neutrino mass matrix $m^2_{\tilde{\nu}}$, restricted to the 2-3 generation subspace, can be written in the fermion mass-diagonal basis as

$$m^2_{\tilde{\nu}} = \begin{pmatrix} \cos\theta_{23} & -\sin\theta_{23} \\ \sin\theta_{23} & \cos\theta_{23} \end{pmatrix} \begin{pmatrix} m_{\tilde{\nu}_2} & 0 \\ 0 & m_{\tilde{\nu}_3} \end{pmatrix} \begin{pmatrix} \cos\theta_{23} & \sin\theta_{23} \\ -\sin\theta_{23} & \cos\theta_{23} \end{pmatrix}, \tag{1}$$

where $m_{\tilde{\nu}_2}$ and $m_{\tilde{\nu}_3}$ are the physical masses of $\tilde{\nu}_2$ and $\tilde{\nu}_3$ respectively. In the following we take the mixing angle θ_{23} and $\Delta m_{23} = |m_{\tilde{\nu}_2} - m_{\tilde{\nu}_3}|$ as free, independent parameters. The same goes for the charged slepton sector, modulo standard LR mixing, where θ_{23} and Δm_{23} are then the corresponding parameters for charged sleptons.[§] If we work in the mass eigenstate basis for all fields, the slepton mixing matrix will appear in interaction vertices of sleptons with leptons and charginos/neutralinos. As a result, the SLFV signals can be looked for in decays of sleptons, for example

$$\begin{aligned} e^+e^- &\to \tilde{\ell}_i^-\tilde{\ell}_i^+ \to \tau^+\mu^-\tilde{\chi}_1^0\tilde{\chi}_1^0, \\ e^+e^- &\to \tilde{\nu}_i\tilde{\nu}_i^c \to \tau^+\mu^-\tilde{\chi}_1^+\tilde{\chi}_1^- \end{aligned} \tag{2}$$

with $i = 2, 3$, or in decays of charginos and/or neutralinos

$$e^+e^- \to \tilde{\chi}_2^+\tilde{\chi}_1^- \to \tau^+\mu^-\tilde{\chi}_1^+\tilde{\chi}_1^- \tag{3}$$

$$e^+e^- \to \tilde{\chi}_2^0\tilde{\chi}_1^0 \to \tau^+\mu^-\tilde{\chi}_1^0\tilde{\chi}_1^0 \tag{4}$$

where $\tilde{\chi}_1^\pm \to \tilde{\chi}_1^0 f\bar{f}'$, and $\tilde{\chi}_1^0$ escapes detection. The signature therefore would be $\tau^\pm\mu^\mp + jets + \not{E}_T$, $\tau^\pm\mu^\mp + \ell + \not{E}_T$, or $\tau^\pm\mu^\mp + \not{E}_T$, depending on hadronic or leptonic $\tilde{\chi}_1^\pm$ decay mode.

Hisano *et al.* [8] first proposed and discussed the search for SLFV signals (through $\tilde{\nu}_\mu - \tilde{\nu}_\tau$ mixing) at an assumed e^+e^- or $\mu^+\mu^-$ linear collider with $\sqrt{s} = 500$ GeV and $\int dt\mathcal{L} = 50\,\text{fb}^{-1}$ considering only the pair-production of sneutrinos and of charged sleptons, eq.(2). The final states, generated by SLFV and analyzed by them, were

$$\text{(A)} : \tau\mu + 4j + \not{E}_T, \qquad \text{(B)} : \tau\mu l + 2j + \not{E}_T, \qquad \text{(C)} : \tau\mu l\bar{l} + 2j + \not{E}_T \tag{5}$$

(with $l = e, \mu$ and$j$ =jets coming from chargino decays) for which the corresponding backgrounds were small and under control. They found that only the signal (A) is viable

[§]One can give a parallel discussion for the e-τ mixing case [12], replacing μ by e everywhere.

in an e^+e^- collider whereas the other two processes would be difficult to observe due to small rates. The observability of signal (B) is better at a $\mu^+\mu^-$ collider, whereas the signal (C) is less promising in this collider too. In their analysis they assumed $m_{\tilde{\chi}_1^\pm} = 100$ GeV.

However, if the chargino $\tilde{\chi}_2^\pm$ is not much heavier, as is the case in a substantial region of the MSSM parameter space, then off-diagonal chargino pair production $e^+e^- \to \tilde{\chi}_1^\pm\tilde{\chi}_2^\mp$ can take place for the linear collider CM energy $\sqrt{s} = 500$ GeV. The heavier chargino can decay via the SLFV chain, eq.(3), and the chargino $\tilde{\chi}_1^\pm\tilde{\chi}_2^\mp$ pair production can also lead to the same final states as in eq.(5) providing a new source for the signal in addition to those discussed in Ref.[8]. Moreover, the production of two charginos in e^+e^- collision has both the s-channel and t-channel exchange contributions and hence expected somewhat larger cross sections at higher collider energies. Other production processes, like $\tilde{\chi}_2^\pm\tilde{\chi}_2^\mp$, $\tilde{\chi}_i^0\tilde{\chi}_j^0$, may also be open at higher energies (depending on the mass pattern) and contribute to the same final states not only via the SLFV mechanisms shown in eqs.(3) and (4), but through lepton flavour conserving decay chains as well. The main difference between our study and that of the Hisano et.al [8] is that realistically we have taken into account additional contributions to SLFV coming from chargino production. We have also considered background from production of supersymmetric particles which were not considered in Ref. [8]. Moreover, since we allow two jets in (A) to overlap, we also consider an important SM background coming from $\bar{t}tg$ production followed by semileptonic top decays. We note that recently possible signals of the SLFV in chain decays of neutralinos produced at the LHC have been discussed [13].

To illustrate the phenomenology of the SLFV process, we estimate the signal and background rates for two representative points [14] in the MSSM parameter space given in terms of two mSUGRA scenarios chosen for detailed case studies at the ECFA/DESY linear collider workshop:

$$\begin{aligned} RR1: &\quad m_0 = 100; \quad M_{1/2} = 200; \quad A_0 = 0; \quad \tan\beta = 3; \quad \mathrm{sgn}(\mu) = + \\ RR2: &\quad m_0 = 160; \quad M_{1/2} = 200; \quad A_0 = 600; \quad \tan\beta = 30; \quad \mathrm{sgn}(\mu) = + \end{aligned} \tag{6}$$

Here the masses and A_0 are in GeV, and standard notation is used. The masses of corresponding chargino, neutralino and slepton states are shown in Table 1 along with the relevant branching ratios which are used in our calculations. The listed branching ratios are for the case of no slepton mixing; the effect of mixing is calculated below. The lightest neutralino $\tilde{\chi}_1^0$ is nearly a bino while $\tilde{\chi}_2^0$ and $\tilde{\chi}_1^\pm$ are largely winos, thereby being almost degenerate. For these MSSM points, the squarks are heavier than 300 GeV.

A glance at Table 1 shows that in the case of RR2 (*i.e.* for large $\tan\beta$) the lightest chargino decays only leptonically (without SLFV it decays into $\chi_1^0\tau\nu_\tau$). As a result, the signature of SLFV in $\tilde{\chi}_2^\pm\tilde{\chi}_1^\mp$ production would be one muon and three taus plus missing energy. Such a signal might be extremely difficult to extract from background with four taus or with two muons and two taus for realistic tau identification efficiencies. This question calls for full experimental simulations which are clearly beyond the scope of our analysis. Since the process in eq.(3) will not contribute to the final states listed in eq.(5), it can be neglected, as done in Ref.[8]. For the case RR1, however, the lightest chargino has a large branching ratio for hadronic decays. Therefore taking into account the process eq.(3) in addition to eq.(2) may significantly improve sensitivity of an e^+e^-

	RR1			RR2		
Particle	Mass	Decay	BR	Mass	Decay	BR
$\tilde{\chi}_1^+$	128	$\tilde{\chi}_1^0 \ell^+ \nu_\ell$	0.15×3	132	$\tilde{\tau}^+ \nu_\tau$	1.0
		$\tilde{\chi}_1^0 q \bar{q}'$	0.56			
$\tilde{\chi}_2^+$	346	$\tilde{\chi}_2^0 W^+$	0.29	295	$\tilde{\chi}_2^0 W^+$	0.31
		$\tilde{\chi}_1^+ Z$	0.22		$\tilde{\chi}_1^+ Z$	0.22
		$\tilde{\chi}_1^+ h$	0.14		$\tilde{\chi}_1^+ h$	0.13
		$\tilde{t}_1 \bar{b}$	0.14		$\tilde{\nu}_\tau \tau^+$	0.07
		$\tilde{\ell}^+ \nu_\ell$	0.04×3		$\tilde{\tau}_2^+ \nu_\tau$	0.08
		$\ell^+ \tilde{\nu}_\ell$	0.03×3		$\tilde{\chi}_1^0 W^+$	0.06
$\tilde{\chi}_1^0$	72			75		
$\tilde{\chi}_2^0$	130	$\tilde{\chi}_1^0 \tau^+ \tau^-$	0.24	133	$\tilde{\tau}^+ \tau^-$	0.50
		$\tilde{\chi}_1^0 e^+ e^-$	0.20		$\tilde{\tau}^- \tau^+$	0.50
		$\tilde{\chi}_1^0 \mu^+ \mu^-$	0.20			
		$\tilde{\chi}_1^0 \nu_\ell \bar{\nu}_\ell$	0.04×3			
$\tilde{\chi}_3^0$	320	$\tilde{\chi}_1^\pm W^\mp$	0.62	273	$\tilde{\chi}_1^\pm W^\mp$	0.54
		$\tilde{\chi}_2^0 Z$	0.20		$\tilde{\chi}_2^0 Z$	0.15
		$\tilde{\chi}_1^0 Z$	0.14		$\tilde{\chi}_1^0 Z$	0.28
$\tilde{\chi}_4^0$	348	$\tilde{\chi}_1^\pm W^\mp$	0.52	293	$\tilde{\chi}_1^\pm W^\mp$	0.52
		$\tilde{\chi}_2^0 h^0$	0.11		$\tilde{\chi}_2^0 h^0$	0.09
		$\tilde{\chi}_1^0 h^0$	0.07		$\tilde{\chi}_1^0 h^0$	0.06
$\tilde{\ell}_L^-$	176	$\tilde{\chi}_1^- \nu_\ell$	0.53	217	$\tilde{\chi}_1^- \nu_\ell$	0.52
		$\tilde{\chi}_2^0 \ell^-$	0.32		$\tilde{\chi}_2^0 \ell^-$	0.34
		$\tilde{\chi}_1^0 \ell^-$	0.15		$\tilde{\chi}_1^0 \ell^-$	0.14
$\tilde{\nu}_\ell$	161	$\tilde{\chi}_1^0 \nu_\ell$	0.48	202	$\tilde{\chi}_1^+ \ell^-$	0.55
		$\tilde{\chi}_2^0 \nu_\ell$	0.12		$\tilde{\chi}_2^0 \nu_\ell$	0.20
		$\tilde{\chi}_1^0 \nu_\ell$	0.40		$\tilde{\chi}_1^0 \nu_\ell$	0.25
$\tilde{\tau}_1^-$	131	$\tilde{\chi}_1^0 \tau^-$	1.00	92	$\tilde{\chi}_1^0 \tau^-$	1.00
$\tilde{\tau}_2^-$	177	$\tilde{\chi}_1^- \nu_\tau$	0.53	209	$\tilde{\chi}_1^- \nu_\tau$	0.38
		$\tilde{\chi}_2^0 \tau^-$	0.31		$\tilde{\chi}_2^0 \tau^-$	0.28
		$\tilde{\chi}_1^0 \tau^-$	0.16		$\tilde{\chi}_1^0 \tau^-$	0.28
$\tilde{\nu}_\tau$	161	$\tilde{\chi}_1^0 \nu_\tau$	0.48	177	$\tilde{\chi}_1^+ \tau^-$	0.49
		$\tilde{\chi}_2^0 \nu_\tau$	0.12		$\tilde{\chi}_2^0 \nu_\tau$	0.17
		$\tilde{\chi}_1^0 \nu_\tau$	0.40		$\tilde{\chi}_1^0 \nu_\tau$	0.33

Table 1: The masses (in GeV) and the branching ratios (only for significant decay modes) for supersymmetric particles which are relevant to our study. No slepton mixing is assumed. ℓ denotes e or μ, and τ unless the entry for τ is explicitly shown. The SUSY parameter points RR1 and RR2 are as specified in eq.(6) [14].

linear collider to SLFV processes. As it turns out that processes with one or both $\tilde{\chi}_1^\pm$ decaying leptonically are overwhelmed by background, in our analyses we consider only signature (A) in eq.(5). Allowing two quark jets to overlap, in the next section we discuss the final states with $\tau^\pm \mu^\mp + \geq 3 jets$ for signal and background processes in scenario RR1.

3 Collider signals

We perform our study of SLFV in a linear collider, such as the proposed TESLA [15], with a CM energy $\sqrt{s} = 500$ and 800 GeV and an integrated luminosity $\int dt\mathcal{L} = 50-1000$ fb^{-1}. To study the signal and as well as corresponding background rates we use simple parton level Monte Carlo simulation, where each parton is treated as a jet. The viability of this SLFV signal is studied both for $\sqrt{s} = 500$ GeV and $\sqrt{s} = 800$ GeV.

(a) $\sqrt{s} = 500$ GeV case:

In this case, given the mass spectrum of Table 1, the off-diagonal $\tilde{\chi}_1^\pm \tilde{\chi}_2^\mp$ pair is the only possibility for the SLFV signal in chargino production. Starting with the $\tilde{\chi}_1^\pm \tilde{\chi}_2^\mp$ state, slepton flavour violation can occur in the heavier chargino $\tilde{\chi}_2^\mp$ long cascade decay chain. The entire decay sequence is shown as follows:

S1: $e^+e^- \to \tilde{\chi}_2^\pm \tilde{\chi}_1^\mp$

$$\begin{aligned} \tilde{\chi}_2^+ &\to \tau^+ \tilde{\nu}_{2,3}, \qquad \tilde{\nu}_{2,3} \to \mu^- \tilde{\chi}_1^+, \qquad \tilde{\chi}_1^+ \to \tilde{\chi}_1^0 + q + \bar{q}', \\ \tilde{\chi}_1^- &\to \tilde{\chi}_1^0 + q + \bar{q}' \end{aligned} \tag{7}$$

S2: $e^+e^- \to \tilde{\chi}_2^\pm \tilde{\chi}_1^\mp$

$$\begin{aligned} \tilde{\chi}_2^+ &\to \mu^+ + \tilde{\nu}_{2,3}, \qquad \tilde{\nu}_{2,3} \to \tau^- \tilde{\chi}_1^+, \qquad \tilde{\chi}_1^+ \to \tilde{\chi}_1^0 + q + \bar{q}', \\ \tilde{\chi}_1^- &\to \tilde{\chi}_1^0 + q + \bar{q}'. \end{aligned} \tag{8}$$

There is, of course, another sequence with the charges reversed. The other process for signal (A), which was discussed in [8], is the following:

S3: $e^+e^- \to \tilde{\nu}_i \tilde{\nu}_i^c$

$$\begin{aligned} \tilde{\nu}_i &\to \tilde{\chi}_1^- \tau^+; \qquad \tilde{\chi}_1^- \to \tilde{\chi}_1^0 + q + \bar{q}'; \\ \tilde{\nu}_i^c &\to \tilde{\chi}_1^+ \mu^-; \qquad \tilde{\chi}_1^+ \to \tilde{\chi}_1^0 + q + q', \end{aligned} \tag{9}$$

where $i = 2, 3$. Notice that in eqs.(7,8) the slepton flavour violating decay occurs in two ways leading to the the same final state so that eventually the signal rate gets doubled.

The cross section corresponding to signal processes S1 and S2 can be written as

$$\sigma(e^+e^- \to \tau\mu + \geq 3jets) \simeq \chi_{23} \sin^2 2\theta_{23} \times \sigma_0 \times \epsilon_{BR} \times \epsilon_{\tau_{id}}, \tag{10}$$

whereas, for S3, it is given by

$$\sigma(e^+e^- \to \tau\mu + \geq 3jets) \simeq \chi_{23}(3 - 4\chi_{23}) \sin^2 2\theta_{23} \times \sigma_0 \times \epsilon_{BR} \times \epsilon_{\tau_{id}}. \tag{11}$$

The SLFV effect is taken into account [7] by the factors $\sin^2 2\theta_{23}$ and

$$\chi_{23} = \frac{x_{23}^2}{2(1 + x_{23}^2)}, \qquad x_{23} = \Delta m_{23}/\Gamma, \tag{12}$$

where Γ is the decay width of the sneutrino, which is 0.42 GeV for our choice of parameter space and assumed to be independent of flavour. The difference between eq.(10) and eq.(11) is due to the correlated slepton pair production in the process S3.

In the above expressions σ_0 is the corresponding sparticle pair-production cross section in e^+e^- collision and ϵ_{BR} is the product of relevant branching ratios for the corresponding decay chains assuming no SLFV. The value of ϵ_{BR} are easily obtained by consulting Table 1. For example for S1 we get $\epsilon_{BR} = 0.0075$ where the factor 2 accounting two possible cases of $\chi_2^\pm\chi_1^\mp$ is included. The other factor, $\epsilon_{\tau_{id}}$, is the τ lepton selection efficiency. In our calculation we have considered decays of the τ through its hadronic decay modes to products such as $\pi\nu_\tau$, $a_1\nu_\tau$ and $\rho\nu_\tau$ with a total branching ratio of 64%. We have normalized final decay distributions appropriately taking the polarization of the τ [16]. Here the τ is mostly left handed as it couples to $\tilde{\chi}_2^\pm$ through gauge interaction, whereas the right handed coupling is suppressed by its mass as it couples through higgsino part of $\tilde{\chi}_2^\pm$. Assuming the τ identification efficiency 0.70 [17] for these decay modes, we get for the parameter $\epsilon_{\tau_{id}} = 0.45$ including its branching ratios to hadronic decay modes. Note that in full MC simulations one could further improve the signal to background ratio by imposing a cut on the impact parameter of the muon since the muon in the background processes comes in most cases from the decay of a τ which travels some distance from the production vertex before it decays [8]. However, we have not used such a cut in the present study.

A point to be noted is that in the chargino decay processes either the τ (eq.7) or the μ (eq.8) is the leading lepton. The energy distribution of each of these leptons is flat between a maximum and a minimum value. This feature will be exploited to suppress possible background.

Since we allow (unlike Ref.[8]) two jets to overlap, the most dominant Standard Model background to the signal $\tau\mu+ \geq 3jets$ comes from

$$e^+e^- \to t\bar{t}g \tag{13}$$

production followed by semileptonic decays of two top quarks. We have computed this process at tree level using MADGRAPH [18] with energy and isolation cuts discussed below. There are also flavour-conserving SUSY processes that contribute significantly to the background. In the following we list those processes with their possible decay chains:

B1: $e^+e^- \to \tilde{\chi}_2^+\tilde{\chi}_1^-$

$$\begin{aligned} \tilde{\chi}_2^+ &\to \tau^+ + \tilde{\nu}_\tau; \qquad \tilde{\nu}_\tau \to \tau^-(\to \mu^-)\tilde{\chi}_1^+; \qquad \tilde{\chi}_1^+ \to \tilde{\chi}_1^0 + q + \bar{q}'; \\ \tilde{\chi}_1^- &\to \tilde{\chi}_1^0 + q + \bar{q}'. \end{aligned} \tag{14}$$

B2: $e^+e^- \to \tilde{\chi}_2^+\tilde{\chi}_1^-$

$$\begin{aligned} \tilde{\chi}_2^+ &\to \tau^+(\to \mu^+) + \tilde{\nu}_\tau; \qquad \tilde{\nu}_\tau \to \tau^-\tilde{\chi}_1^+; \qquad \tilde{\chi}_1^+ \to \tilde{\chi}_1^0 + q + \bar{q}'; \\ \tilde{\chi}_1^- &\to \tilde{\chi}_1^0 + q + \bar{q}'. \end{aligned} \tag{15}$$

B3: $e^+e^- \to \tilde{\nu}_i\tilde{\nu}_i^c$

$$\begin{aligned} \tilde{\nu}_i &\to \tilde{\chi}_1^-\tau^+; \qquad \tilde{\chi}_1^- \to \tilde{\chi}_1^0 + q + \bar{q}'; \\ \tilde{\nu}_i^c &\to \tilde{\chi}_1^+\tau^-(\to \mu^-); \qquad \tilde{\chi}_1^+ \to \tilde{\chi}_1^0 + q + \bar{q}'. \end{aligned} \tag{16}$$

B4: $e^+e^- \to \tilde{\tau}_2^+\tilde{\tau}_2^-$

$$\begin{aligned} \tilde{\tau}_2^+ &\to \tau^+\tilde{\chi}_2^0; \qquad \tilde{\chi}_2^0 \to \tilde{\chi}_1^0\tau^+(\to jets)\tau^-(\to \mu^-); \\ \tilde{\tau}_2^- &\to \nu_\tau\tilde{\chi}_1^-; \qquad \tilde{\chi}_1^- \to \tilde{\chi}_1^0 + q + \bar{q}'. \end{aligned} \tag{17}$$

In eq.(17) the $\tilde{\tau}_2$ is the heavier physical state after the mixing between $\tilde{\tau}_L$ and $\tilde{\tau}_R$. Notice that in all background cases B1–B4 the μ comes from τ decay after the $\tau\tau X$ events are produced.

(b) $\sqrt{s} = 800$ GeV case:

Because of the higher energy, many new sparticle production channels containing heavier states of charginos and neutralinos open now, contributing both to signal and background processes. Cross sections of these are typically $\simeq \mathcal{O}(\text{fb})$. Note that the $\tilde{\nu}_i\tilde{\nu}_i^c$ pair-production will be suppressed at higher $\sqrt{s}$ since it is an s-channel mediated process. As far as our signal is concerned, a new source is the diagonal heavier chargino($\tilde{\chi}_2^\pm\tilde{\chi}_2^\mp$) pair-production. One of the $\tilde{\chi}_2^\pm$ will decay through the flavour violating mode as shown in eqs.(7,8) while the other $\tilde{\chi}_2^\mp$ will decay sequentially to 2 jets and $\not{E}_T$ as shown below:

S4: $e^+e^- \to \tilde{\chi}_2^\pm\tilde{\chi}_2^\mp$

$$\begin{aligned} \tilde{\chi}_2^+ &\to \tau^+\tilde{\nu}_{2,3}, \qquad \tilde{\nu}_{2,3} \to \mu^-\tilde{\chi}_1^+, \qquad \tilde{\chi}_1^+ \to \tilde{\chi}_1^0 + q + \bar{q}', \\ \tilde{\chi}_2^- &\to \tilde{\chi}_1^- Z \to \tilde{\chi}_1^0 q\bar{q}'\,\nu\bar{\nu}, \;\; \text{or} \;\; \tilde{\chi}_2^- \to \tilde{\chi}_2^0 W^- \to \tilde{\chi}_1^0\nu\bar{\nu}\,q\bar{q}' \end{aligned} \tag{18}$$

S5: $e^+e^- \to \tilde{\chi}_2^\pm\tilde{\chi}_2^\mp$

$$\begin{aligned} \tilde{\chi}_2^+ &\to \mu^+ + \tilde{\nu}_{2,3}, \qquad \tilde{\nu}_{2,3} \to \tau^-\tilde{\chi}_1^+, \qquad \tilde{\chi}_1^+ \to \tilde{\chi}_1^0 + q + \bar{q}', \\ \tilde{\chi}_2^- &\to \tilde{\chi}_1^- Z \to \tilde{\chi}_1^0 q\bar{q}'\,\nu\bar{\nu}, \;\; \text{or} \;\; \tilde{\chi}_2^- \to \tilde{\chi}_2^0 W^- \to \tilde{\chi}_1^0\nu\bar{\nu}\,q\bar{q}' \end{aligned} \tag{19}$$

In the case of background processes, there are also new sources which cannot be neglected. We find four additional processes leading to the same final states:

B5: $e^+e^- \to \tilde{\chi}_2^+\tilde{\chi}_2^-$

$$\begin{aligned} \tilde{\chi}_2^- &\to \tilde{\chi}_1^- Z, \; \tilde{\chi}_1^- h^0 \to \tilde{\chi}_1^0\tau\nu_\tau q\bar{q}, \\ \tilde{\chi}_2^+ &\to \tilde{\chi}_1^+ Z, \; \tilde{\chi}_1^+ h^0 \to \tilde{\chi}_1^0\mu\nu_\mu q\bar{q} \end{aligned} \tag{20}$$

B6: $e^+e^- \to \tilde{\chi}_3^0\tilde{\chi}_2^0$

$$\begin{aligned} \tilde{\chi}_3^0 &\to \tilde{\chi}_1^+ W \to \tilde{\chi}_1^0 q\bar{q}' q\bar{q}', \\ \tilde{\chi}_2^0 &\to \tilde{\chi}_1^0\tau^+\tau^-(\to \mu). \end{aligned} \tag{21}$$

B7: $e^+e^- \to \chi_2^0\chi_4^0$

$$\begin{aligned} \tilde{\chi}_2^0 &\to \chi_1^0\tau^+\tau^-(\to \mu^-), \\ \tilde{\chi}_4^0 &\to \chi_1^\pm W^\mp \to \chi_1^0 q\bar{q}'\,q\bar{q}' \end{aligned} \tag{22}$$

B8: $e^+e^- \to \chi_3^0\chi_4^0$

$$\begin{aligned} \tilde{\chi}_3^0 &\to \chi_1^\pm W^\mp \to \chi_1^0\mu\nu\,q\bar{q}', \\ \tilde{\chi}_4^0 &\to \chi_1^\pm W^\mp \to \chi_1^0\tau\nu\,q\bar{q}' \end{aligned} \tag{23}$$

4 Expected signal and background rates

We have used the following selection cuts for our events using simple parton level simulation:

1. The τ and μ are selected with the restriction $|\cos\theta_\mu| < 0.99$ and $|\cos\theta_\tau| < 0.96$. This cut has been applied to avoid leptons which are very close to the beam direction [17]. We have put a selection cut on $E_\tau > 2$ GeV.

2. The selection cut on the missing energy is applied as $|\cos\vec{\theta}_{miss}| < 0.90$ in order to avoid missing energy which is along the beam pipe [17].

3. We select leptons to be isolated if the visible energy around the cone $\Delta R = 0.4$ is less than the maximum (10% of E_ℓ, 1 GeV). Here $\Delta R = \sqrt{\Delta\phi(\ell,j)^2 + \Delta\eta(\ell,j)^2}$, with $\Delta\phi(\ell,j)$ and $\Delta\eta(\ell,j)$ being the differences of azimuth and pseudorapidity respectively, between any lepton and one of the jets.

4. As mentioned before, we have treated partons as jets without including showering and fragmentation effects. We consider two jets as isolated if they pass the selection cuts $\Delta\tilde{R} = \sqrt{\Delta\phi(j,j)^2 + \Delta\eta(j,j)^2} > 0.6$. Here $\Delta\phi(j,j)$ and $\Delta\eta(j,j)$ are the differences of azimuth and pseudorapidity respectively between any two jets. We accept those jets which are not too close to the beam pipe, *i.e.* with $|\cos\theta_{jet}| < 0.95$, and have energy $E_j > 0.05\,(\sqrt{s} - 2m_t)$. The last cut originates from the necessity to regulate the IR singularity of the QCD background process, eq.(13).

5. The final muon energy cut is applied to reduce the backgrounds of eqs.(14–17) and eqs.(21–23). For these background processes, the μ always comes from τ decay. Therefore, this μ is expected to have less energy than the μ of the signal process. For example, in the case of the signal process S1, the maximum and minimum energies of the τ and the μ are given by:

$$\begin{aligned} E_\tau^{(max,min)} &= E_\tau^{rest}(1 \pm \beta_{\tilde{\chi}})\gamma_{\tilde{\chi}} \\ E_\mu^{(max,min)} &= E_\mu^{rest}(1 \pm \beta_{\tilde{\nu}})\gamma_{\tilde{\nu}} \end{aligned} \tag{24}$$

where

$$E_\tau^{rest} = \frac{m_{\tilde{\chi}_2^+}^2 - m_{\tilde{\nu}}^2}{2m_{\tilde{\chi}_2^+}}; \quad E_\mu^{rest} = \frac{m_{\tilde{\nu}}^2 - m_{\tilde{\chi}_1^+}^2}{2m_{\tilde{\nu}}} \tag{25}$$

are the τ and μ energies in the rest frames of $\tilde{\chi}_2^+$ and $\tilde{\nu}$, respectively, and β's and γ's are the respective CM boost parameters. For the case of eq.(8), τ and μ have to be interchanged in the above expressions. These maximum and minimum energies depend on massive particles involved in the initial and final states of two body decay subprocesses. Therefore, putting a cut on the energy of μ, such as $E_\mu > 25$ GeV, reduces substantially these backgrounds.

Note that the dominant SM background, eq.(13), contains two b-quark jets coming from top decays in contrast to the signal processes which contain jets initiated by light

	S1	S2	S3	B1	B2	B3	B4
0	118	118	1080	20	20	183	173
1	118	105	1035	18	18	176	147
2	98	98	945	17	17	161	134
3	84	84	765	14	14	122	121
4	57	71	661	9	12	107	99
5	57	71	508	2	8	27	38

Table 2: The signal and background cross sections (in ab) for $\sqrt{s} = 500$ GeV and the reference point RR1 after each set of cuts as discussed in the text. The branching ratios and $\epsilon_{\tau_{id}}$ factors are included.

quarks. Therefore, further background suppression could be achieved by imposing a veto to the events containing tagged b jets. However, we have not used this criteria in our analysis as it requires a detailed MC simulation including detector effects which is beyond the scope of the present paper.

Applying the selection cuts, as described by 1-5 above, we have estimated the signal and background rates for the scenario RR1.

(a) $\sqrt{s} = 500$ GeV case:

In Table 2 we show the expected cross sections for the signal and background processes (all cross sections are in ab). The numbers in the first row correspond to the raw production cross sections including branching ratio and τ identification factors, whereas the numbers in consecutive rows show the effect of kinematic cuts described above. Therefore, by using eq.(10) the total signal cross sections for S1 and S2 turn out to be:

$$\sigma(e^+e^- \to \tau\mu + \geq 3jets) \simeq \chi_{23} \sin^2 2\theta_{23} \times 0.128 \ \text{ fb}, \tag{26}$$

whereas for signal S3, using eq.(11), it is

$$\sigma(e^+e^- \to \tau\mu + \geq 3jets) \simeq \chi_{23}(3 - 4\chi_{23}) \sin^2 2\theta_{23} \times 0.508 \ \text{ fb}. \tag{27}$$

In comparison, the total cross section for the background is 0.282 fb which includes 0.075 fb from SUSY processes listed in Table 2 and 0.207 fb from the QCD process eq.(13) after all cuts. Using Poisson distributions, the significance is $\sigma_d = \frac{N}{\sqrt{N+B}}$ where N and B is the number of signal and background events respectively for a given luminosity. In Fig.1 we have shown the region (to the right of the curve) in the $\Delta m_{23} - \sin 2\theta_{23}$ plane that can be explored or ruled out at a 3σ level by the linear collider of energy 500 GeV for the given integrated luminosity. We have drawn the contours for three luminosity options, namely 50 fb^{-1}, 500 fb^{-1} and 1000 fb^{-1}, whereas the dashed line shows the reach of the process $\tilde{\nu}_i\tilde{\nu}_i^c$ alone, eq.(9), using our cuts and assuming luminosity of 500 fb^{-1}. Comparing the dashed line with line B we see that that the chargino contribution, eq.(7,8) increases the sensitivity range to $\sin^2\theta_{23}$ by 10-20% while the sensitivity to Δm_{23} does not change appreciably.

(b) $\sqrt{s} = 800$ GeV case:

	S1	S2	S3	S4	S5	B1	B2	B3	B4	B5	B6	B7	B8
0	108	108	720	53	53	18	18	115	138	131	98	56	147
1	101	101	720	51	51	17	17	107	125	123	89	54	138
2	91	88	630	39	45	16	16	100	117	112	80	52	125
3	78	78	360	38	38	13	13	61	95	102	80	51	115
4	25	31	130	38	37	5	5	22	36	102	15	10	53
5	25	31	108	30	37	1	4	7	18	70	4	4	32

Table 3: The signal and background cross sections (in ab) for $\sqrt{s} = 800$ GeV and the reference point RR1 after each set of cuts as discussed in the text. The branching ratios and $\epsilon_{\tau_{id}}$ factors are included.

Here we have generated events using our parton level simulation and applied the same selection criteria, as discussed earlier. Our estimated signal and background rates are given in Table 3. We find that the total signal rate in this case is 0.231 fb where the contribution from both off diagonal and as well as diagonal chargino production is 0.123 fb and from sneutrino production it is 0.108 fb. On the other hand, the background cross section is 0.315 fb, which includes 0.145 fb from SUSY processes, as given by Table 3, and 0.17 fb from the QCD process eq.(13). Using eqs.(10) and (11), we can isolate the region which can be probed or ruled out at a linear collider CM energy of 800 GeV. This is shown for two luminosity options in Fig. 2 in the same plane as in Fig.1; the luminosity of 50 fb^{-1} is not sufficient to exclude any region in the figure for this CM energy.

5 Conclusions

In this paper we have discussed the detection of SLFV at a future e^+e^- linear collider. We assumed the dominant $\nu_\mu - \nu_\tau$ mixing as suggested by super-Kamiokande atmospheric results. In the MSSM, the SLFV in left-handed sleptons is induced radiatively, leading to second and third generation slepton mixing, and to a final state with $\tau\mu + \geq 3jets + \not{E}_T$ in e^+e^- collisions as a most interesting signal. The physics potential of exploring SLFV at an e^+e^- LC has been analyzed for two reference points in the supersymmetry parameter space: RR1 with low $\tan\beta = 3$, and RR2 with high $\tan\beta = 30$, and for two CM energies $\sqrt{s} = 500$ and 800 GeV. The novel feature of our analysis is the inclusion of diagonal and non-diagonal chargino and neutralino pair production processes to the SLFV signal and background. The calculations have been performed at the parton-level Monte Carlo simulations including realistic experimental cuts. The SM background from the QCD process $e^+e^- \to t\bar{t}g$ has been included as well.

For the low $\tan\beta = 3$ scenario (RR1) we find that, though the sneutrino pair production process is the dominant one, the chargino pair production processes are not negligible contributing more to the signal than to the background. As a result, the sensitivity of the linear collider to the SLFV in the parameter space of $\Delta m_{23} - \sin 2\theta_{23}$ plane is increased. We also find that operating at $\sqrt{s} = 500$ GeV, where only non-diagonal $\tilde{\chi}_1^\pm \tilde{\chi}_2^\mp$ chargino pairs can be produced, is the most optimal for the RR1 scenario. Increasing the CM energy to 800 GeV reduces the sensitivity mainly due to the decrease of sneutrino cross

section not compensated by opening $\tilde{\chi}_2^{\pm}\tilde{\chi}_2^{\mp}$. The latter also contributes significantly to the background (B5) at $\sqrt{s} = 800$ GeV, thereby diluting the SLFV signal at that energy. Thus $\sqrt{s} = 800$ GeV does not seem to be a viable CM energy option for studying SLFV in the RR1 scenario.

For the high $\tan\beta = 30$ scenario (RR2), only the $\mu + 3\tau + \not{E}_T$ final states might signal SLFV processes. However, only detailed Monte Carlo simulations including all experimental aspects may tell us if such final states can realistically be reconstructed.

Acknowledgements
We thank M. Drees, H. Martyn, M.M. Nojiri, X. Tata and P. Zerwas for helpful discussions. MG is also thankful to V.Ravindran for fruitful discussion. The authors acknowledge the hospitality of the DESY theory group. MG was supported by Alexander Von Humboldt Foundation during the initial phase of this work. The work of JK has partially been supported by the KBN Grant No. 2 P03B 060 18. Work supported in part by the European Commission 5-th framework contract HPRN-CT-2000-00149.

References

[1] Y. Fukuda *et al.*, Phys. Rev. Lett. **82** (1999) 2644 [hep-ex/9812014]; T. Toshito, talk given at the XXX International Conference on High Energy Physics (2000), Osaka.

[2] M. Apollonio *et al.*, Phys. Lett. B **420** (1998) 397 [hep-ex/9711002]; F. Boehm *et al.*, Phys. Rev. Lett. **84** (2000) 3764 [hep-ex/9912050].

[3] Y. Fukuda *et al.*, Phys. Rev. Lett. **82** (1999) 1810 [hep-ex/9812009]; Y. Takeuchi, talk given at the XXX International Conference on High Energy Physics (2000), Osaka.

[4] M. L. Brooks *et al.*, Phys. Rev. Lett. **83** (1999) 1521 [hep-ex/9905013]; S. Ahmed *et al.*, Phys. Rev. D **61** (2000) 071101 [hep-ex/9910060].

[5] J. Ellis *et al.*, Eur. Phys. J. C **14** (2000) 319 [hep-ph/9911459]; . L. Feng, Y. Nir and Y. Shadmi, Phys. Rev. D **61** (2000) 113005 [hep-ph/9911370].

[6] N.V. Krasnikov, *Mod. Phys. Lett.* **A9** (1994) 791.

[7] N. Arkani-Hamed, J. L. Feng, L. J. Hall and H. Cheng, Phys. Rev. Lett. **77** (1996) 1937 [hep-ph/9603431], Nucl. Phys. B **505** (1997) 3 [hep-ph/9704205].

[8] . Hisano, M. M. Nojiri, Y. Shimizu and M. Tanaka, Phys. Rev. D **60** (1999) 055008 [hep-ph/9808410].

[9] M. Gell-Mann, P. Ramond and R. Slansky, in *Supergravity, Proc. Supergravity Workshop at Stony Brook* (ed. P. van Nieuwenhuizen and D.Z. Freedman, North Holland, Amsterdam 1979). T. Yanagida, *Proc. Workshop on the Unified Theory and the Baryon Number in the Universe* (ed. O. Sawada and A. Sugamoto, KEK 1979-18).

[10] F. Borzumati and A. Masiero, Phys. Rev. Lett. **57** (1986) 961; L. J. Hall, V. A. Kostelecky and S. Raby, Nucl. Phys. B **267** (1986) 415; L. Hall, V. Kostelecky and S. Raby, *Nucl. Phys.* **B267** (1986) 415. J. Hisano, T. Moroi, K. Tobe, M. Yamaguchi and T. Yanagida, Phys. Lett. B **357** (1995) 579 [hep-ph/9501407].

[11] J. Hisano, T. Moroi, K. Tobe and M. Yamaguchi, Phys. Rev. D **53** (1996) 2442 [hep-ph/9510309].

[12] D. Nomura, hep-ph/0004256.

[13] I. Hinchliffe and F. E. Paige, hep-ph/0010086.

[14] 2nd Joint ECFA/DESY Study on *Physics and Detectors for a Linear Electron-Positron Colliders*, http:// www.desy.de/conferences/ecfa-desy-lc98.html.

[15] E. Accomando *et al.*, Phys. Rept. **299** (1998) 1 [hep-ph/9705442].

[16] B. K. Bullock, K. Hagiwara and A. D. Martin, Nucl. Phys. B **395** (1993) 499.

[17] H.U.Martyn, private communication.

[18] T. Stelzer and W. F. Long, Comput. Phys. Commun. **81** (1994) 357 [hep-ph/9401258].

Figure 1: The significance contours (for the SUSY point RR1 mentioned in the text) in $\Delta m_{23} - \sin 2\theta_{23}$ plane for $\sqrt{s}$ =500 GeV and for different luminosity options, contours A, B and C being for 50 fb^{-1}, 500 fb^{-1} and 1000 fb^{-1}, respectively. The dashed line is for only $\tilde{\nu}\tilde{\nu}^c$ contribution with luminosity 500 fb^{-1}. The upper-right side of these contours can be explored or ruled out at the 3σ level.

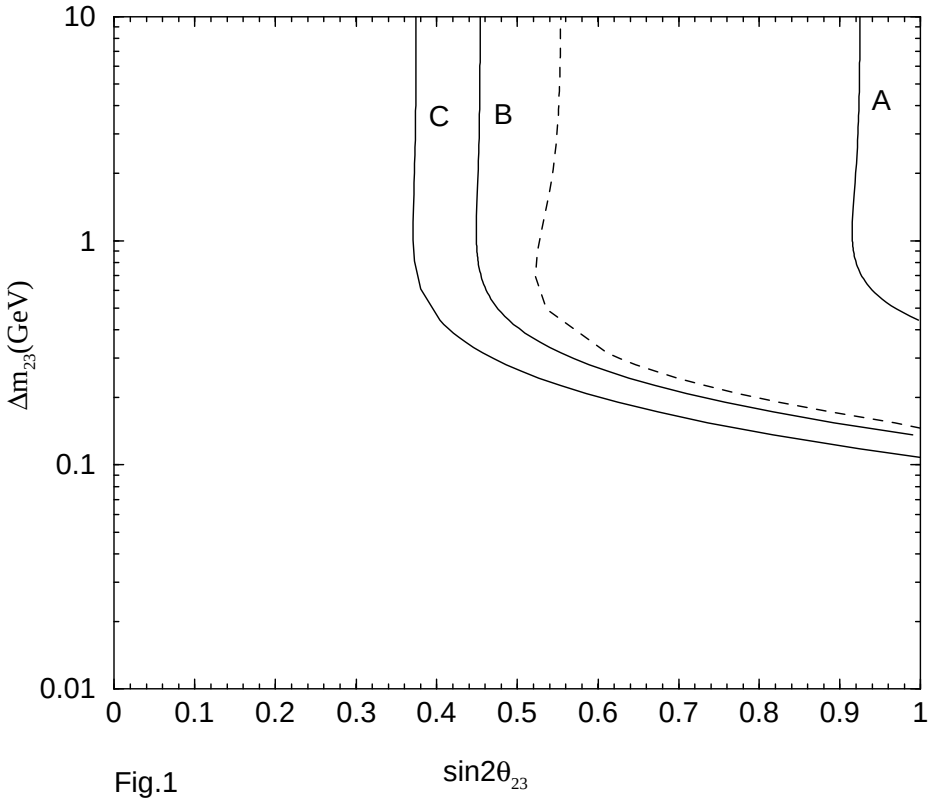

Fig.1

Figure 2: The same as in Fig.1 for $\sqrt{s}$ =800 GeV and two luminosities 500 fb^{-1} and 1000 fb^{-1}

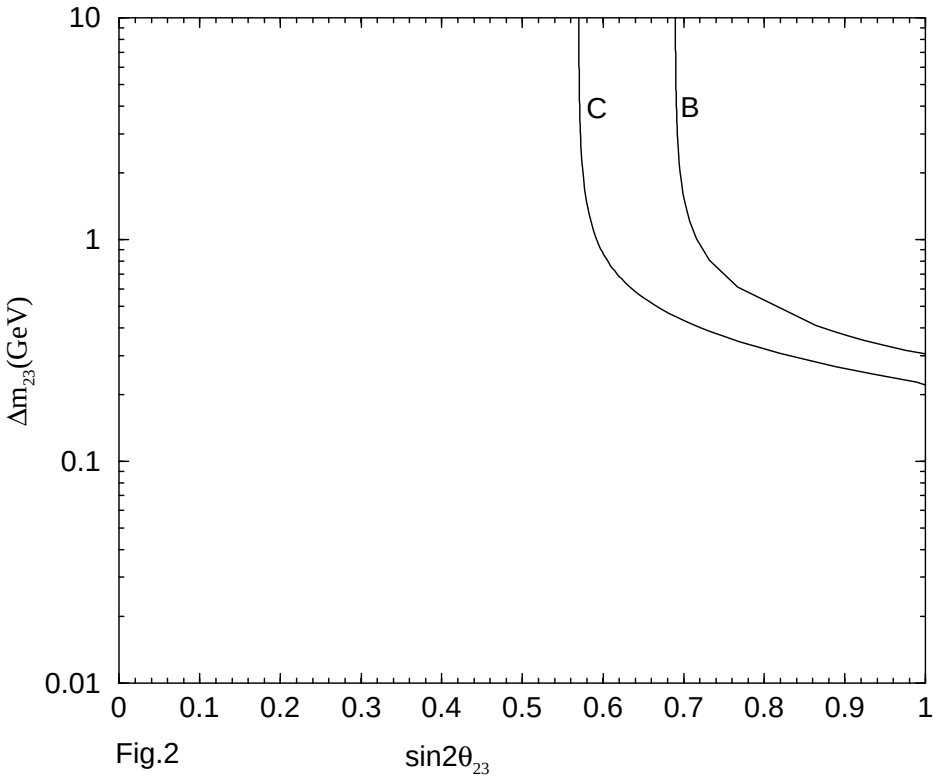

Fig.2